

Experimental Observation of Dynamical Behavior of Self-mixing by Doppler Feedback in Microchip Nd:YAG Laser

Chen-An Chan,¹ Ming-Chi Lu,¹ Feng-Wei Tsai,¹ Yan-Lin Zhong,¹
Tang-Yi Tsai,² Chun-Shen Hsu,² Bo-Yi Li,² Zai-Xing Zheng,²
Tzu-Fang Hsu,³ Chia-Ju Liu,² and Ming-Chung Ho^{1*}

¹Department of Physics, National Kaohsiung Normal University,
No. 62, Shenghong Rd., Yanchao District, Kaohsiung City 824, Taiwan, ROC

²Graduate Institute of Science Education & Environmental Education, National Kaohsiung Normal University,
No. 62, Shenghong Rd., Yanchao District, Kaohsiung City 824, Taiwan, ROC

³Department of Applied Physics, National Pingtung University of Education,
No. 4-18, Minsheng Rd., Pingtung City 900, Taiwan, ROC

(Received November 30, 2018; accepted July 10, 2019)

Keywords: feedback light injection, diode-pumped lasers, laser Doppler velocimetry, chaos, self-mixing

We present our experimental observations of self-mixing laser Doppler velocimetry (LDV) with a laser-diode-pumped microchip Nd:YAG laser. Periodic intensity fluctuations were detected by local maximum analysis, and the real-time temporal waveforms were observed using an oscilloscope. A rotary motor with an aluminum foil surface was used in the laser-diode-pumped Nd:YAG system to generate a feedback beam with Doppler shift frequency. Since a low Doppler shift frequency perturbed this laser system, the observed waveforms existed as pulselike oscillation groups, which presented chaotic oscillations. When the Doppler shift frequency gradually increased, the number of peaks in each pulselike oscillation group decreased, and the self-mixing system was gradually manipulated using the Doppler shift frequency. As the Doppler shift frequency gradually increased to 43 kHz, the output signal was dominated by the Doppler shift frequency such that the oscillation behaved similarly to a periodic fluctuation.

1. Introduction

Because of the complex dynamical properties of lasers, the instabilities of nonlinear optical resonators and lasers, and the fluctuations of pumping modulation have continuously attracted attention over the past decade.^(1,2) We can obtain a chaotic output from a diode-pumped-microchip laser by pump modulation, loss modulation, or weak feedback light injection. In a Nd-doped laser with a thin cavity, the photolifetime is short and the fluorescence lifetime is so large that the fluorescent-to-photolifetime ratio is large. A laser material with a longer fluorescence lifetime would be more suitable for further enhancement of sensitivity and responsiveness to external modulation or feedback light injection.⁽³⁾ Lang and Kobayashi

*Corresponding author: e-mail: t1603@nknuc.nknu.edu.tw
<https://doi.org/10.18494/SAM.2019.2213>

proposed chaotic instabilities in the output of a laser manipulated by optical feedback in 1980,⁽⁴⁾ and other study interests focused on the instabilities of lasers with delayed feedback, including external cavity feedback, polarization feedback, backscattering feedback, and Doppler feedback.^(5–12) Upon the occurrence of the effect of the Doppler shift feedback, the chaotic instabilities of the system would be strongly affected by Doppler shift frequencies. Hence, the synchronizations between two or more coupled Doppler feedback systems are of relevant research interest.⁽¹³⁾

In this study, we investigated the oscillation behavior and bifurcation diagram of a route to chaos of a diode laser with optical feedback.^(14–16) In general, turning a table or rotating a circular paper sheet stuck to a rotating metal plate resulted in a weak backscattering beam injected into the laser system, which was a feedback beam with Doppler shift frequency.^(9–12) In this paper, we present a new method of generating a Doppler shift feedback beam, by which the laser beam was directly reflected by aluminum foil stuck on a rotary motor. We discuss the instabilities of the output laser signal caused by the directly reflected beam with Doppler shift frequency rather than the scattered beam. By analyzing the local maximum method and time interval diagram, we observed the corresponding intensity fluctuation of Doppler shift frequency. In addition, by plotting a diagram of Doppler shift frequencies at different motor frequencies, we successfully observed a series of global scale multiple relaxation oscillation (RO) behavior. That is, our experimental device for self-mixing laser Doppler velocimetry (LDV) could be used as a Doppler speedometer and could be a potential sensitivity sensor device for velocity.

2. Experimental Setup

The experimental setup of self-mixing by Doppler shift feedback in a laser-diode-pumped microchip Nd:YAG laser system is schematically illustrated in Fig. 1. The Nd:YAG crystal was a rod of 5 mm length and 1 mm diameter, and both ends of the crystal were coated with

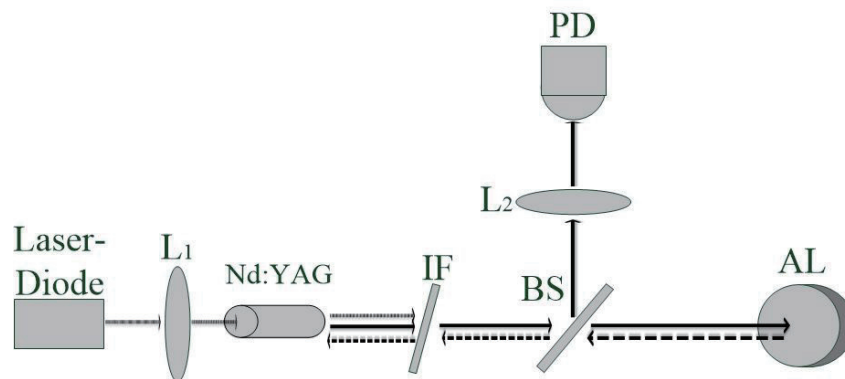


Fig. 1. Experimental setup of self-mixing by Doppler shift feedback in laser-diode-pumped microchip Nd:YAG (YAG) laser system: L₁ and L₂, focusing lenses; IF, interference filter; BS, beam splitter; AL, aluminum foil; PD, photodiode.

dielectric mirrors, in which the reflectances of the front and back surfaces at 1064 nm were 99 and 95%, respectively. A laser diode (Melles Griot, 06 DLD 105) with a wavelength of 808 nm served as the pumping source, which was controlled at an operating temperature of 25 °C to stabilize the RO frequencies of device outputs by using a temperature controller (Thorlabs, TED 200 C). The oscillation threshold P_{th} of the pumped Nd:YAG laser beam was 104.6 mW and the slope efficiency was 24%. A single-mode oscillation was obtained below $\omega = P/P_{1st} = 1.107$ ($P =$ pumping power), and multimode oscillations were observed at higher pumping levels. The corresponding power spectrum peak at 77 kHz was the RO frequency of this system. To prevent the effect of the residual beam of 808 nm wavelength, the pumped laser beam was allowed to pass through the interference filter (IF) so that only the dynamics of the pumped beam of 1064 nm wavelength would be discussed here. The pumped laser beam was split into two beams by the beam splitter (BS). One beam was focused on the aluminum foil so that the laser beam would be fed back into the laser crystal to perturb the output oscillation. The temporal waveform was measured by the PD (New Focus, 1811FS) with a bandwidth of 125 MHz. An oscilloscope (Tektronix, DPO 4054B) with a sample rate of 2.5 Gs/s read the signal from the photodiode (PD) to obtain the temporal waveform of the oscillation of the laser beam. The fast Fourier transform of the temporal waveform was evaluated to obtain its power spectrum.

3. Experimental Results

The aluminum foil in this experiment was stuck on a rotational motor and controlled using the motor velocity so that the Doppler shift frequency of the feedback beam was in the range from 11 to 43 kHz. The temporal waveforms and corresponding power spectra of the laser system at Doppler shift frequencies of 11, 19, 28, and 43 kHz are shown in Fig. 2. When the

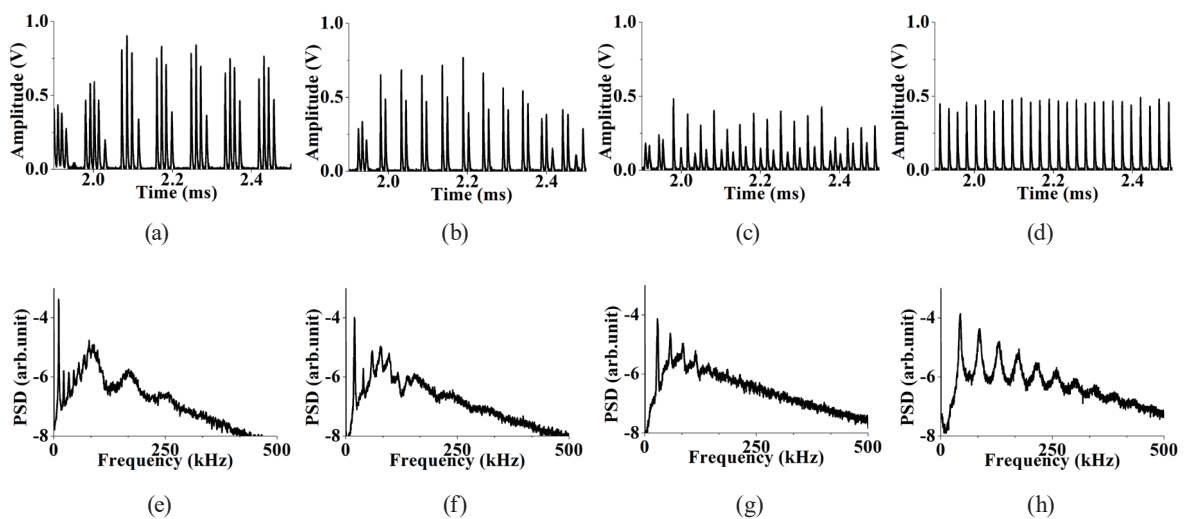


Fig. 2. Temporal waveforms and power spectra of the laser system obtained at Doppler shift frequencies of (a) 11, (b) 19, (c) 28, and (d) 43 kHz and (e)–(h) corresponding power spectra.

Doppler shift frequency was controlled at 11 kHz, the temporal waveforms of the output laser signal shown in Fig. 2(a) were pulselike oscillations and the power spectra were observed to exhibit a chaotic bandwidth. The peak of 11 kHz in Fig. 2(e) indicates that the RO frequency of the system corresponds to 0.088 ms, which could be evaluated using the duration between group pulses in Fig. 2(a). The power spectrum of the RO in Fig. 2(e) is also accompanied by some regular small oscillations, which correspond to the pulse duration between four pulses in each pulselike oscillation group. Hence, it was shown that, although the oscillations obtained in a long duration of 4 ms were chaotic, the pulselike oscillation groups in a short duration of 0.6 ms were observed to exhibit a certain regular behavior.

As the Doppler shift frequency increased, the number of peaks in each pulselike oscillation group decreased. At the Doppler shift frequency of 19 kHz, the temporal waveform shown in Fig. 2(b) depicts that the number of peaks in each pulselike oscillation group decreased to two.

However, not all the pulselike oscillation groups consisted of two peaks; some of the groups consisted of only one peak. When the Doppler shift frequency increased, the number of pulselike oscillation groups with only one peak increased continuously. As shown in Fig. 2(c), at the Doppler shift frequency of 28 kHz, the number of pulselike oscillation groups with only one peak exceeded that of pulselike oscillation groups with two peaks. The power spectra in Figs. 2(g) and 2(f) depict that the oscillation at 28 kHz is more periodic than that at 19 kHz. This indicates that the regularity in oscillation was destroyed and the manipulation of the Doppler shift frequency gradually became strong when the Doppler shift frequency increased. When the Doppler shift frequency was higher than 28 kHz, each pulselike oscillation group consisted of only one peak. Hence, the fluctuation of the system at the Doppler shift frequency of 43 kHz shown in Fig. 2(d) behaved similarly to the periodic oscillation, indicating that the output of the microchip Nd:YAG laser system was almost dominated by the Doppler shift frequency. The curve of the power spectrum in Fig. 2(h) also showed that the oscillation behaved similarly to periodic fluctuations.

To statistically analyze the oscillation behavior with a Doppler shift signal, the time interval between adjacent peaks was evaluated even up to a maximum motor frequency of 100 Hz, as shown in Fig. 3. At each motor frequency, the shorter-time-interval region indicates the time interval between the adjacent peaks in each pulselike oscillation group, while the larger-time-interval region indicates the time interval between adjacent oscillation groups, which is related to the RO of the laser output. When the motor frequency was lower than 22 Hz, the shorter-time-interval region was observed. However, the shorter-time-interval region vanished when the motor frequency was higher than 22 Hz. This proved that the oscillation in the pulselike oscillation group consisted of more than two peaks when the motor frequency was lower than 22 Hz, and that the oscillations had only one RO region when the motor frequency was higher than 22 Hz. Note that the time interval behavior of a motor frequency higher than 22 Hz also depicted that the RO was manipulated by Doppler shift frequency. The regularity in only one RO region varied into a two-periodic-oscillation behavior when the motor frequency was higher than 30 Hz. Moreover, the number of RO regions became more complex indicating a three- or four- or multirelaxation oscillation behavior when the motor frequency was higher than 40 Hz or even 60 Hz.

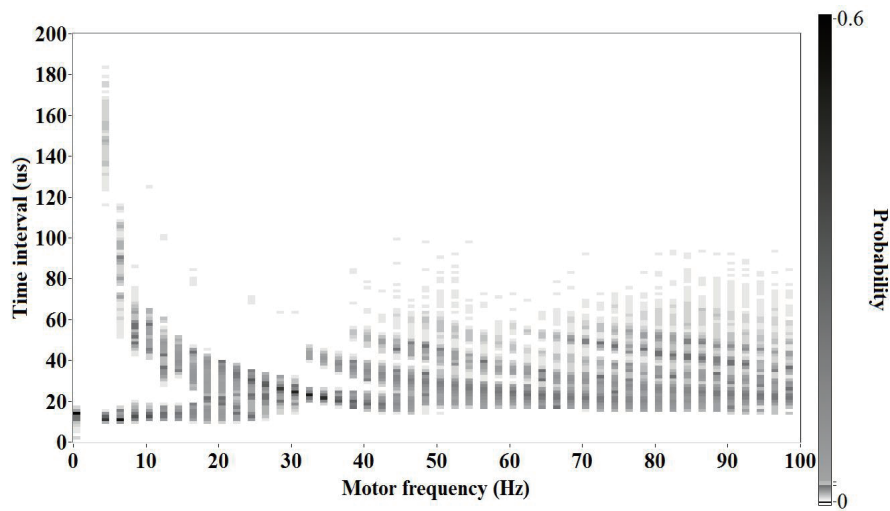


Fig. 3. Time interval between adjacent peaks with Doppler shift frequency.

4. Discussion

However, the diagram in Fig. 3 could show us the existence of the pulselike oscillation group, but could not provide any information to distinguish the situations in Figs. 2(b) and 2(c). The probability as a function of the time interval between adjacent peaks could provide us this information, as shown in Fig. 4. At the Doppler shift frequencies of 11 and 19 kHz, as shown in Figs. 4(a) and 4(b), respectively, the maximum probability in the shorter-time-interval region was higher than that in the longer-time-interval region, indicating that most peaks existed in the groups. At Doppler shift frequencies of 23 and 31 kHz in Figs. 4(c) and 4(d), respectively, the maximum probability in the shorter-time-interval region became lower than that in the longer-time-interval region. This indicates that, although the pulselike oscillation group still existed, the number of groups with only one peak gradually increased with the Doppler shift frequency. This also proves that the degree of manipulation increased with Doppler shift frequency. Finally, as the Doppler shift frequency tuned to 43 kHz, as shown in Fig. 4(e), only the probability in the longer-time-interval region existed. This depicts that the laser output behaved similarly to the periodic oscillation dominated by the Doppler shift frequency. Moreover, as the Doppler frequency continuously increased, the phenomena of growth and decline of the probability of time interval of the Doppler shift frequencies were observed. That is, the second cycle of probability competition was observed at Doppler shift frequencies of 46, 59, 67, and 79 kHz, as shown in Figs. 4(f) to 4(i), and Figs. 4(j) to 4(l) showed the third cycle of probability competition observed at Doppler shift frequencies of 90, 114, and 130 kHz, respectively.

We carefully labeled the corresponding power spectrum peak in the motor frequency range from zero to 100 Hz, as shown in Fig. 5. Figure 5 also shows that the oscillation in the pulselike oscillation group consisted of more than two peaks when the motor frequency was lower than 22 Hz. Moreover, the periodic oscillation behavior varied from one to two, the number of RO regions became more complex, and the number of periods of RO increased to three and even

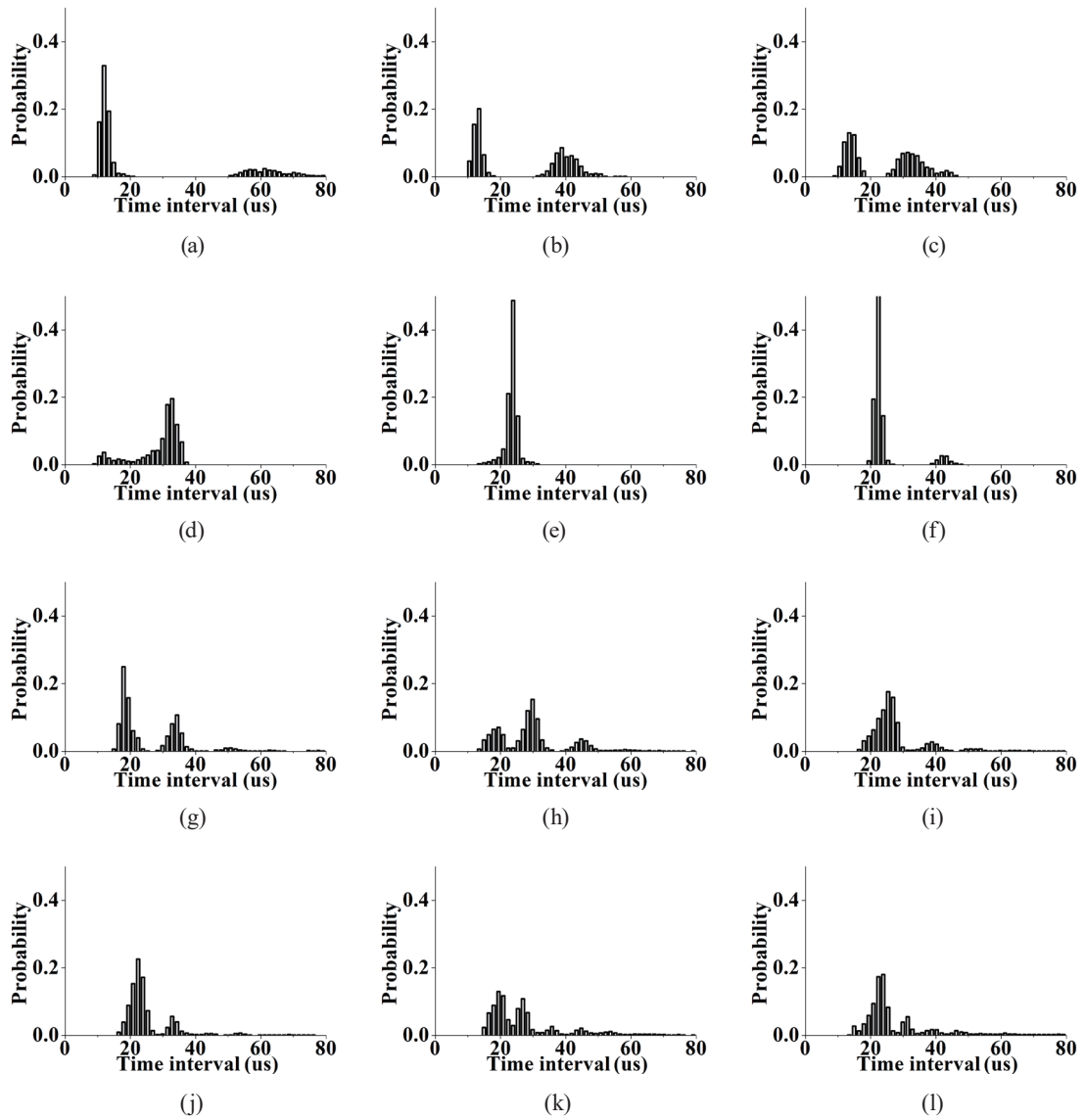


Fig. 4. Probability as function of time interval between adjacent peaks of the system at Doppler shift frequencies of (a) 11, (b) 19, (c) 23, (d) 31, (e) 43, (f) 46, (g) 59, (h) 67, (i) 79, (j) 90, (k) 114, and (l) 130 kHz, where the motor frequencies are 8, 14, 16, 22, 30, 32, 40, 46, 54, 60, 76, and 88 Hz, respectively.

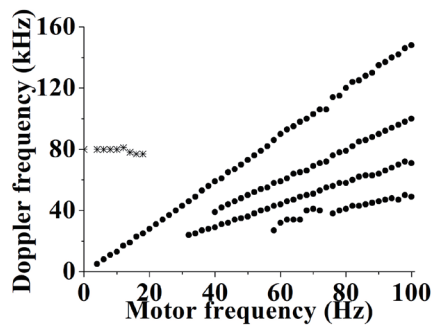


Fig. 5. Multi-Doppler frequency vs motor frequency.

four when the motor frequency increased to 30, 40, and even 60 Hz. That is, various transitional behaviors of multirelaxation oscillation were observed in this study; no such behaviors were observed in other self-mixing Doppler laser systems.

5. Conclusions

A new method of generating a Doppler shift feedback beam directly reflected by aluminum foil stuck on a rotary motor of self-mixing LDV with a diode-pumped laser single-mode microchip Nd:YAG laser was presented. As a weak Doppler shift frequency perturbed this laser system by external feedback, the temporal waveform of its output signal resulted in pulslike oscillation groups, and the power spectrum indicated that laser oscillations were chaotic. When the Doppler shift frequency gradually increased, the number of peaks in each pulslike oscillation group decreased, and the self-mixing system was gradually manipulated using the Doppler shift frequency. As the Doppler shift frequency gradually increased to 43 kHz, the output signal was dominated by the Doppler shift frequency such that the oscillation behaved similarly to a periodic fluctuation. Additionally, the number of periods of RO increased to three and even four when the motor frequency increased to 30, 40, and even 60 Hz, indicating the various transitional behaviors of multirelaxation oscillation.

References

- 1 K. Otsuka, J. Y. Ko, T. Kubota, S. L. Hwang, T. S. Lim, J. L. Chern, B. A. Nguyen, and P. M. Mandel: *Opt. Lett.* **26** (2001) 1060. <https://doi.org/10.1364/OL.26.001060>
- 2 C. H. Lin, C. T. Kuo, T. F. Hsu, H. Jan, S. Y. Han, M. C. Ho, and I. M. Jiang: *Phys. Lett. A* **376** (2012) 1295. <https://doi.org/10.1016/j.physleta.2012.02.037>
- 3 T. Ohtomo and K. Otsuka: *Jpn. J. Appl. Phys.* **48** (2009) 070212. <https://doi.org/10.1143/JJAP.48.070212>
- 4 R. Lang and K. Kobayashi: *IEEE J. Quantum Electron.* **QE-16** (1980) 347. <https://doi.org/10.1109/JQE.1980.1070479>
- 5 K. Otsuka, J.-Y. Ko, J.-L. Chern, K. Ohki, and H. Utsu: *Phys. Rev. A* **60** (1999) 3389. <https://doi.org/10.1103/PhysRevA.60.R3389>
- 6 T. S. Lim, T. H. Yang, J. L. Chern, and K. Otsuka: *IEEE J. Quantum Electron.* **37** (2001) 1215. <https://doi.org/10.1109/3.945328>
- 7 M. A. Arteaga, O. Parriaux, L. A. Manuel, H. Thienpont, and K. Panajotov: *Appl. Phys. Lett.* **90** (2007) 121104. <https://doi.org/10.1063/1.2714301>
- 8 W. M. Wang, W. J. O. Boyle, K. T. V. Grattan, and A. W. Palmer: *Appl. Opt.* **32** (1993) 1551. <https://doi.org/10.1364/AO.32.001551>
- 9 E. T. Shimizu: *Appl. Opt.* **26** (1987) 4541. <http://doi.org/10.1364/AO.26.004541>
- 10 K. Otsuka: *IEEE J. Quantum Electron.* **QE-15** (1979) 655. <https://doi.org/10.1109/JQE.1979.1070053>
- 11 K. Otsuka: *Appl. Opt.* **33** (1994) 1111. <https://doi.org/10.1364/AO.33.001111>
- 12 A. Uchida, T. Sato, M. Takeoka, and F. Kannari: *Jpn. J. Appl. Phys.* **36** (1997) 912. <https://doi.org/10.1143/JJAP.36.L912>
- 13 K. Otsuka, D. Pieroux, J. Y. Wang, and P. Mandel: *Opt. Lett.* **22** (1997) 516. <https://doi.org/10.1364/OL.22.000516>
- 14 A. Uchida, T. Sato, and F. Kannari: *Opt. Lett.* **23** (1998) 460. <http://doi.org/10.1364/OL.23.000460>
- 15 C. Juang, S. M. Chang, N. K. Hu, C. Lee, and W. W. Lin: *Jpn. J. Appl. Phys.* **44** (2005) 7827. <https://doi.org/10.1143/JJAP.44.7827>
- 16 J. Mørk, J. Mark and B. Tromborg: *Phys. Rev. Lett.* **65** (1990) 1999. <https://doi.org/10.1103/PhysRevLett.65.1999>